*Sci. and Cult.* 90 (5–6) : 235-238 (2024)

# Lattice Dynamical Investigation of Raman and IR Wave Numbers at the Zone Center of Orthorhombic Perovskite $LuFeO_3$

***Abstract*: Herein, we have investigated the Raman and infrared wave numbers of orthorhombic perovskite $LuFeO_3$ by using normal coordinate analysis in light of a short-range valence band force-field model. For the calculation of zone center phonons, we have employed 9 stretching and 7 bending force constants in the Wilson GF matrix method. Our calculated wave numbers agree well with the observed wave numbers. The Raman wave numbers have been assigned to their specific mode of vibrations. The infrared wave numbers have been calculated and assigned. The potential energy distribution has also been determined to signify the contribution of the force constants toward the Raman and infrared wave numbers.**

**Keywords:** Raman and Infrared wave numbers, Orthorhombic perovskite, Lattice dynamics, Force Constant

Rare-earth orthoferrites have the general chemical formula $RFeO_3$, where R is the rare-earth ion ($R^{3+}$), having an orthorhombically distorted perovskite structure. It was first discovered and some of its magnetic properties were characterized in the late 1940s[1]. The prospective applications of rare-earth orthoferrites in contemporary optoelectronic and spintronic devices serve as a driving force behind their investigation[2-3]. They are the most suited multiferroics with magneto-electric (ME) coupling at room temperature since they exhibit both ferroelectric and magnetic properties together[4-6]. Among the multiferroics, $LuFeO_3$ has attracted much attention because of the discovery of multiferroicity in thin film and bulk forms[7-8]. Additionally, $LuFeO_3$ shows captivating magnetic properties, including canted anti-ferromagnetism and spin reorientation transition (SRT)[9-11]. The SRT is observed only for those crystals wherein the $R^{3+}$ ions carry a magnetic moment[12-13].

An investigation of Raman and Infrared wave numbers is useful for identifying and characterizing the crystalline samples. The polarized Raman spectra of $LuFeO_3$ were recorded by Venugopalan *et al.*[14] who assigned the observed modes of $LuFeO_3$. In this work, we have attempted to study the zone center phonons in $LuFeO_3$ using a short-range valance band force-field model, based on the atomic vibrations. Most of the wave numbers corresponding to Raman modes were assigned by us. Our calculated values resemble well, with those of the experimental ones observed by other researchers[14,17-18]. Additionally, we estimated the infrared (IR) wave numbers and examined the potential energy distribution to identify the significance of the force constants (FCs) toward the Raman and IR wave numbers.

***Structure:*** At room temperature, the structure of $LuFeO_3$ is orthorhombic (space group:Pbnm). The unit cell of the crystal with sub-units corresponding to the ideal cubic perovskite unit cell is shown in Figure 1. The lattice parameters are, a = 5.213 Å, b = 5.547 Å, c = 7.565 Å, $\alpha = \beta = \gamma = 90^{o}$; V=218.75 $Å^3$ and Z=4[12-15]. The Lu atom is at the center of a distorted octahedron formed by O atoms. The group theoretical analysis using the standard correlation method[16] provides the irreducible representation of the vibration modes of four different atoms lying in different Wyckoff sites of the Bravais unit cell. Table 1 shows the site symmetry, atomic coordinates[15], and the phonon contribution at the Γ-point.

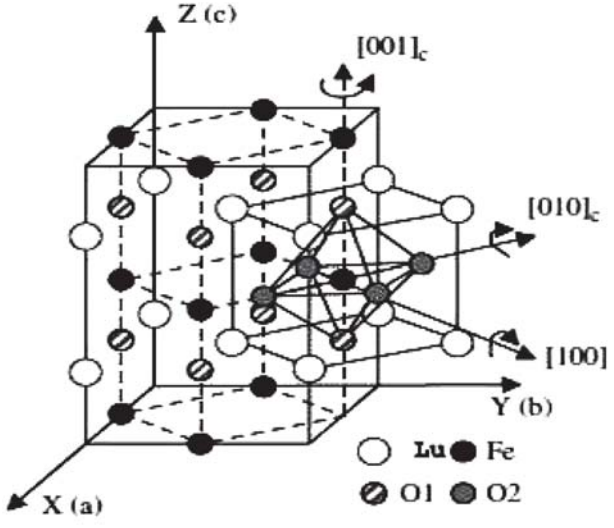


**Fig. 1:** Crystal structure of orthorhombic $LuFeO_3$ having space group Pbnm. The unit cell along with sub-units corresponding to the ideal cubic perovskite unit cell is shown.

**The journal is in the category 'Group A' of UGC-CARE list and falls under the broad category of Multidisciplinary Sciences covering the areas Arts and Humanities, Science and Social Sciences.**

The total irreducible representation of the crystal at the Γ-point of the Brillouin zone consists of 60 zone-center normal modes and is given by

$$\Gamma = 7A_g + 7B_{1g} + 5B_{2g} + 5B_{3g} + 8A_u + 8B_{1u} + 10B_{2u} + 10B_{3u} \quad (1)$$

Out of these normal modes, only 25 modes are active in the infrared absorption region:

$\Gamma_{infrared} = 7B_{1u} \oplus 9B_{2u} \oplus 9B_{3u}$. The acoustic branch of the crystal vibrations is represented by three IR modes ($B_{1u} \oplus B_{2u} \oplus B_{3u}$), which are connected to three degrees of translation mode of the unit cell as a whole. Raman activity is represented by 24 phonon modes: $\Gamma_{Raman} = 7A_g \oplus 7B_{1g} \oplus 5B_{2g} \oplus 5B_{3g}$. The remaining modes ($8A_u$) are optically inactive.

***Theory:*** Based on Cartesian symmetry coordinates, lattice dynamical computations were performed by using the Wilson GF matrix method. Solutions were found for the eigenvalue equation given by $|F - G^{-1}\lambda| = 0$, where $G^{-1}$ is the kinetic energy matrix and $F$ is a matrix of force constants coming from potential energy matrix contributions. $\lambda$ is the eigenvalue given by $\lambda = 4\pi^2 c^2 \bar{\nu}^2$ where $\bar{\nu}$ is the wave number. The short-range stretching interactions with valence and repulsive force constants *Ki, Fi,* and bending force constants *Hi* are used to represent the matrix *F*. In our present calculations with the short-range valance-bond force field model, we have used nine valence force constants: $K_1$(Fe-O(1)), $K_2$(Fe-O(2)), $K_3$(Fe-O(2)), $K_4$ (Lu-O(1)), $K_5$(Lu-O(1)), $K_6$ (Lu-O(1)), $K_7$ (Lu—O(2)), $K_8$ (Lu-O(2)) and $K_9$ (Lu-O(2)) and seven bending force constants: $H_{10}$(O(1)-Fe-O(2)), $H_{11}$(O(1)-Lu-O(1)), $H_{12}$(O(1)-Lu-O(1)), $H_{13}$(O(1)-Lu-O(1)), $H_{14}$(O(2)-Lu-O(2)), $H_{15}$(O(2)-Lu-O(1)) and $H_{16}$(O(2)-Lu-O(2)). The various force constants along with interatomic distances, angles, and coordination numbers are shown in Table 2.

***Results and Discussion:*** The optical spectra appear due to internal vibrations of Lu, Fe, and O ions forming distorted $FeO_6$ octahedra and $LuO_{12}$ dodecahedra in the perovskite structure. The interactions between atoms in a crystal lattice are described by force constants which are basic parameters in lattice dynamics. They play a crucial role in vibrational property prediction. In this work, we have calculated the Raman as well as the IR modes using the Force Constants given in Table 2.

In the realm of lattice dynamics, Raman and infrared (IR) spectroscopy are used for examining the vibrational characteristics of the materials. They offer important insights about a material's vibrational modes, their symmetries, etc. We have theoretically found out the Raman wave numbers. The calculated wave numbers (Table 3) are

**Table 1: Site symmetry, atomic coordinates for $LuFeO_3$[15], and the phonon contribution at the Γ-point**

| Atoms | Sites | X | Y | Z | Phonon contribution |
|---|---|---|---|---|---|
| Lu | 4c | 0.9800 | 0.0715 | 0.2500 | $2A_g + 2B_{1g} + B_{2g} + B_{3g} + A_u + B_{1u} + 2B_{2u} + 2B_{3u}$ |
| Fe | 4b | 0 | 0.5 | 0 | $3A_u + 3B_{1u} + 3B_{2u} + 3B_{3u}$ |
| O(1) | 4c | 0.1199 | 0.4539 | 0.2500 | $2A_g + 2B_{1g} + B_{2g} + B_{3g} + A_u + B_{1u} + 2B_{2u} + 2B_{3u}$ |
| O(2) | 8d | 0.6893 | 0.3071 | 0.0621 | $3A_g + 3B_{1g} + 3B_{2g} + 3B_{3g} + 3A_u + 3B_{1u} + 3B_{2u} + 3B_{3u}$ |

**Table 2: Inter-atomic force-constant (FC) values for $LuFeO_3$.**

| Force Constant | Bond Angle between atoms | Coordination number | Bond distance (Å)/ angle (°) | Force Constant values (N/cm) |
|---|---|---|---|---|
| $K_1$ | Fe – O(1) | 8 | 2.0082 | 0.708 |
| $K_2$ | Fe – O(2) | 8 | 1.9972 | 0.059 |
| $K_3$ | Fe – O(2) | 8 | 2.0239 | 0.920 |
| $K_4$ | Lu – O(1) | 4 | 2.2430 | 0.458 |
| $K_5$ | Lu – O(1) | 4 | 3.1946 | 0.317 |
| $K_6$ | Lu – O(1) | 4 | 3.5026 | 0.291 |
| $K_7$ | Lu – O(2) | 8 | 2.2250 | 1.219 |
| $K_8$ | Lu – O(2) | 8 | 2.4546 | 0.284 |
| $K_9$ | Lu – O(2) | 8 | 3.5996 | 1.460 |
| $H_{10}$ | O(2) – Fe – O(1) | 8 | 92.311 | 0.123 |
| $H_{11}$ | O(2) – Fe – O(2) | 8 | 89.947 | 0.080 |
| $H_{12}$ | O(1) – Lu – O(1) | 4 | 120.756 | 0.693 |
| $H_{13}$ | O(1) – Lu – O(1) | 4 | 149.008 | 0.089 |
| $H_{14}$ | O(2) – Lu – O(2) | 8 | 55.797 | 0.322 |
| $H_{15}$ | O(2) – Lu – O(1) | 8 | 72.377 | 0.242 |
| $H_{16}$ | O(2) – Lu – O(2) | 8 | 74.698 | 0.237 |

**Table 3: Experimentally observed[14,17,18] and calculated wave numbers ($cm^{-1}$) of $LuFeO_3$ along with PED % (only two major contributions)**

| Species | $LuFeO_3$ | | |
|---|---|---|---|
| | Observed wave numbers | Our calculated wave numbers | Two major contributions in percentage as per PED |
| $A_g$ (1) | 606 | 600 | $K_7$ (27%) + $K_9$ (26%) |
| $A_g$ (2) | - | 565 | $K_9$ (19%) + $H_{12}$ (43%) |
| $A_g$ (3) | 427 | 415 | $K_3$ (26%) + $H_{14}$ (34%) |
| $A_g$ (4) | 244 | 255 | $K_4$ (43%) + $K_5$ (21%) |
| $A_g$ (5) | 226 | 226 | $K_3$ (10%) + $K_8$ (58%) |
| $A_g$ (6) | 158 | 162 | $K_7$ (26%) + $K_9$ (27%) |
| $A_g$ (7) | 111 | 113 | $K_4$ (22%) + $K_5$ (31%) |
| $B_{1g}$(1) | - | 622 | $K_7$ (31%) + $K_9$ (36%) |
| $B_{1g}$(2) | 516 | 512 | $H_{12}$ (58%) + $H_{15}$ (13%) |
| $B_{1g}$(3) | 446 | 447 | $K_3$ (19%) + $H_{14}$ (19%) |
| $B_{1g}$(4) | - | 330 | $K_4$ (31%) + $K_6$ (26%) |
| $B_{1g}$(5) | 226 | 231 | $K_8$ (58%) + $H_{11}$ (23%) |
| $B_{1g}$(6) | 158 | 151 | $K_4$ (28%) + $H_{14}$ (20%) |
| $B_{1g}$(7) | 134 | 126 | $K_7$ (29%) + $K_9$ (23%) |
| $B_{2g}$(1) | 606 | 620 | $K_7$ (33%) + $K_9$ (36%) |
| $B_{2g}$(2) | 453 | 463 | $K_1$ (21%) + $H_{14}$ (34%) |
| $B_{2g}$(3) | - | 410 | $K_1$ (51%) + $H_{15}$ (18%) |
| $B_{2g}$(4) | 226 | 225 | $K_8$ (56%) + $H_{11}$ (22%) |
| $B_{2g}$(5) | - | 88 | $H_{11}$ (23%) + $H_{16}$ (37%) |
| $B_{3g}$(1) | - | 582 | $K_7$ (37%) + $K_9$ (42%) |
| $B_{3g}$(2) | - | 475 | $K_1$ (36%) + $H_{14}$ (31%) |
| $B_{3g}$(3) | - | 329 | $K_1$ (46%) + $K_3$ (36%) |
| $B_{3g}$(4) | - | 225 | $K_8$ (58%) + $H_{16}$ (15%) |
| $B_{3g}$(5) | - | 151 | $K_7$ (45%) + $K_9$ (30%) |
| $B_{1u}$(1) | - | 619 | $K_7$ (34%) + $K_9$ (40%) |
| $B_{1u}$(2) | - | 472 | $K_1$ (74%) + $H_{14}$ (17%) |
| $B_{1u}$(3) | - | 420 | $K_3$ (49%) + $H_{14}$ (15%) |
| $B_{1u}$(4) | - | 258 | $K_8$ (38%) + $H_{10}$ (15%) |
| $B_{1u}$(5) | - | 186 | $H_{10}$ (18%) + $H_{11}$ (27%) |
| $B_{1u}$(6) | - | 111 | $H_{14}$ (67%) + $K_1$ (9%) |
| $B_{1u}$(7) | - | 82 | $K_2$ (58%) + $H_{11}$ (25%) |
| $B_{2u}$(1) | - | 639 | $K_7$ (23%) + $K_9$ (28%) |
| $B_{2u}$(2) | - | 564 | $K_6$ (22%) + $H_{12}$ (39%) |
| $B_{2u}$(3) | - | 419 | $K_2$ (67%) + $K_3$ (16%) |
| $B_{2u}$(4) | - | 328 | $K_6$ (30%) + $H_{13}$ (25%) |
| $B_{2u}$(5) | - | 275 | $K_7$ (18%) + $H_{11}$ (41%) |
| $B_{2u}$(6) | - | 213 | $K_1$ (83%) + $K_3$ (8%) |
| $B_{2u}$(7) | - | 190 | $K_2$ (22%) + $K_3$ (69%) |
| $B_{2u}$(8) | - | 142 | $K_5$ (33%) + $K_9$ (33%) |
| $B_{2u}$(9) | - | 81 | $K_8$ (22%) + $H_{14}$ (21%) |
| $B_{3u}$(1) | - | 623 | $K_3$ (20%) + $K_7$ (42%) |
| $B_{3u}$(2) | - | 540 | $K_7$ (27%) + $H_{13}$ (30%) |
| $B_{3u}$(3) | - | 448 | $K_2$ (63%) + $K_3$ (14%) |
| $B_{3u}$(4) | - | 348 | $K_4$ (16%) + $K_6$ (70%) |
| $B_{3u}$(5) | - | 251 | $K_3$ (33%) + $H_{11}$ (56%) |
| $B_{3u}$(6) | - | 222 | $K_1$ (90%) + $H_{10}$ (6%) |
| $B_{3u}$(7) | - | 185 | $K_7$ (21%) + $K_9$ (32%) |
| $B_{3u}$(8) | - | 167 | $K_8$ (27%) + $H_{16}$ (35%) |
| $B_{3u}$(9) | - | 86 | $K_8$ (51%) + $H_{16}$ (20%) |

compared with the experimentally determined Raman modes[18]. There is a good agreement between the calculated and experimental Raman modes. We have also calculated the IR modes using the short-range valence band force-field model. The potential energy distributions (PED%) for each mode are investigated to determine the contribution of different FCs to various frequencies. The potential energy distribution plays a critical role in lattice dynamics since it facilitates the understanding of the vibrational behaviour of atoms inside a crystal lattice.

Two major contributions of the force constants towards PED are shown in Table 3. The force constants, $K_7$ and $K_9$, consisting of the Lu-O(2) bond contribute dominantly to the high-frequency modes at 606 $cm^{-1}$ of $A_g$ mode, 622 $cm^{-1}$ of $B_{1g}$ mode, 606 $cm^{-1}$ of $B_{2g}$ mode, 582 $cm^{-1}$ of $B_{3g}$ mode, 619 $cm^{-1}$ of $B_{1u}$ mode, and 639 $cm^{-1}$ of $B_{2u}$ mode. A contribution of the force constants, $K_3$ and $K_7$, is found for 623 $cm^{-1}$ of $B_{3u}$ mode.

The force constants, $H_{12}$ and $H_{14}$, have the utmost significance for the frequencies 565 $cm^{-1}$ of $A_g$ mode, 516 $cm^{-1}$ of $B_{1g}$ mode, 453 $cm^{-1}$ of $B_{2g}$ mode, 475 $cm^{-1}$ of $B_{3g}$ mode, and 564 of $B_{2u}$ mode. It is noticed from the theoretical calculations that Lu-O(1) and Lu-O(2) bonds are responsible for the low-frequency wave numbers 111 $cm^{-1}$ of $A_g$ mode, 134 $cm^{-1}$ of $B_{1g}$ mode, 88 $cm^{-1}$ of $B_{2g}$ mode, 151 $cm^{-1}$ of $B_{3g}$ mode, 111 $cm^{-1}$ of $B_{1u}$ mode, 81 $cm^{-1}$ of $B_{2u}$ mode, and 86 $cm^{-1}$ of $B_{3u}$ mode.

***Conclusions:*** In summary, we have successfully employed the short-range force field model to assign the Raman and infrared modes of orthorhombic (space group:

Pbnm) perovskite $LuFeO_3$ at the Γ-point. The lattice dynamics calculations are performed on the basis of SRFCM by utilizing Wilson's GF matrix method. It is an elegant and effective approach to investigate and assign the vibrational spectra of an arbitrary crystalline structure by producing a complete set of eigenvectors and their respective eigenvalues. Herein, our calculation includes nine short-range bond stretching and seven angle-bending FCs to parameterize the nearest-neighbour interactions within the framework of normal coordinate analysis. The calculated optical modes are fitted well with the available experimental results reported in the literature. The potential energy distribution has also been investigated to identify the significance of the force constants (FCs) toward the Raman and IR wave numbers.

This research contributes significantly to the scientific community by providing a thorough grasp of the vibrational properties of $LuFeO_3$, a material of interest because of its prospective uses in various technological fields. The findings not only validate the theoretical study but also shed light on the structural dynamics of the sample, which could be crucial for designing various devices based on its unique properties. The vibrational properties of $LuFeO_3$ significantly influence its electronic and magnetic characteristics, which are essential for applications in spintronics and optoelectronics.


## *Acknowledgements*

The authors express their heartfelt gratitude to Professor H.C. Gupta of IITD for his bountiful support and express thankfulness to the University of Kalyani for providing infrastructural facilities. ❐



**NANDALAL DAS[a,b,†]**
**JYOTI SAHA[c]**
**YATRAMOHAN JANA[a*]**

[*a] Department of Physics,
University of Kalyani,
Kalyani 741235, Nadia, W.B., India

[b] Department of Physics,
Mahadevananda Mahavidyalaya,
Barrackpore, 700120, North 24Pgs., W.B., India

[c] Department of Physics,
Taki Government College,
Taki, 743429, North 24 Pgs., W.B., India

[†]Corresponding author: nandalalpd@gmail.com



*Received: 20 February, 2024*

*Revised: 20 March, 2024*

*Re-Revised: 12 April, 2024*



1. H. Forestier and G. Guiot-Guillain, *Compt. rend.* **230**, (1950).
2. W. Eerenstein, N. D. Mathur, and J. F. Scott, *Nature* **442** (7104), 759-765 (2006).
3. R. V. Pisarev, A. S. Moskvin, A.M. Kalashnikova, and T. H. M. Rasing, *Phys. Rev. B***79** (23),(2009).
4. Y. Tokunaga, N. Furukawa, H. Sakai, Y. Taguchi, T. Arima, and Y. Tokura, *Nat. Mater* **8**(7), 558-562 (2009).
5. S. Acharya, J. Mondal, S. Ghosh, S. K. Roy, and P. K. Chakrabarti, *Mater. Lett.* **64**(3), 415-418 (2010).
6. N. A. Hill and A. Filippetti, *J.Magn. Magn. Mater.***242**(2), 976-979 (2002).
7. W. Wang, J. Zhao, W. Wang, Z. Gai, N. Balke, M. Chi, H. Lee, T. Wang, L. Zhu, X. Cheng, D. Keavney, J. Yi, T. Ward, P. Snijders, H. Christen, W. Wu, J. Shen, X.Xu,*Phys. Rev. Lett.* **110**(23), (2013).
8. U. Chowdhury, S. Goswami, D. Bhattacharya, J. Ghosh, S. Basu, and S. Neogi, *Appl. Phys. Lett.* **105**(5), (2014).
9. R. White, *J. Appl. Phys.* **40**(3), 1061-1069 (1969).
10. J.H. Lee, Y.K. Jeong, J.H. Park, M.A. Oak, H.M. Jang, J.Y. Son, J.F. Scott. *Phys. Rev. Lett.* **107**(11), (2011).
11. M. Shang, C. Zhang, T. Zhang, L. Yuan, L.Ge, H. Yuan, S. Feng, *Appl. Phys. Lett.* **102**(6), (2013).
12. D. Treves, *J. Appl. Phys.* **36**(3), 1033-1039 (1965).
13. H. Horner and C. M. Varma, *Phys. Rev. Lett.* **20**(16), 845-846 (1968).
14. S. Venugopalan and M. M. Becker, *J. Chem. Phys.***93** (6), 3833-3836 (1990).
15. M. Marezio, J. P. Remeika, and P. D. Dernier, *Acta. Cryst. B***26**(12), 2008-2022 (1970).
16. W. G. Fateley, N. T. McDevitt, and F. F. Bentley, *Appl. Spectrosc.* **25**(2), 155-173 (1971).
17. L. P. Zhu, H. M. Deng, L. Sun, J. Yang, P. X. Yang, and J. H. Chu, *Ceram. Int.* **40**(1), 1171-1175 (2014).
18. P. Suresh, K. Vijaya Laxmi, and S. Anil, *Nucleation and Atmospheric Aerosols*, **1728**(1), (2016).